Time-Stretch Spectroscopy Based on Laser Cavity Tuning With a Dual-Function Delay Line

Srikamal J. Soundararajan and Lingze Duan, *Senior Member, IEEE*

***Abstract*— Time-stretch spectroscopy has established as a viable technique with high resolution and single-shot capability. However, it generally requires ultra-wideband photodetectors and electronics, and its performance is often restricted by a fundamental tradeoff between spectral resolution and signal-to-noise ratio. Here, we report a time-stretch spectrometer based on the concept of optical sampling by laser cavity tuning. A kilometer-scale dual-function fiber-optic link serves as both a pulse stretcher and a long delay line in an imbalanced Mach–Zehnder interferometer. Measurement results based on several device and atomic samples are presented. Theoretical forms of the total spectral range and spectral resolution are derived and compared with experimental data. A spectral resolution as small as 8 GHz has been achieved. Resolution-limiting factors are discussed and possible solutions are presented.**

***Index Terms*— Delay lines, laser tuning, optical fiber dispersion, signal sampling, spectroscopy.**

I. Introduction

TIME-STRETCH spectroscopy has attracted a lot of interest in recent years due to its simplicity and single-shot ability [1]–[8]. The method utilizes a dispersive medium, e.g., optical fibers, to map the spectra of ultrafast optical pulses into time sequences of power readings, which can be directly probed by photodetectors [2]. A drawback of this approach, however, is the reliance of spectral resolution on the speeds of detectors and supporting electronics [3]. As a result, fast photodetectors and sampling oscilloscopes with tens-of-GHz bandwidths are often required, limiting the applicability and scalability of the technique in field applications [6], [7]. Additionally, a tradeoff between spectral resolution and signal-to-noise ratio (SNR) has become a fundamental roadblock in performance optimization [8]. Although the problem can be partially addressed by means of distributed Raman amplification [6], [8], the added cost and complexity offset some of the benefits, nonetheless restricting the feasibility of the scheme.

Meanwhile, an alternative technique called time-wavelength optical sampling (TWOS) has recently been proposed [9]. This new method seeks to eliminate the need for high-speed detectors and electronics by introducing the concept of *optical sampling* into a time-stretch scheme [10]. It can also mitigate the tradeoff between spectral resolution and SNR via the measurement of cross-correlation function (rather than direct power measurement). In addition, the recent advance in sampling techniques based on optical frequency combs has facilitated the development of *real-time* TWOS spectroscopy. Concepts such as asynchronous optical sampling (ASOPS) [11] and optical sampling by cavity tuning (OSCAT) [12]–[17] can be readily applied on a TWOS platform to achieve rapid spectral scans. For instance, we have previously demonstrated a TWOS spectrometer based on the OSCAT method with a 150-Hz updating rate and a 60-nm spectral coverage [9].

While this preliminary study proves the concept of OSCAT-based TWOS spectroscopy, the full potential of the technique has not been adequately explored. Only 38 m pulse-stretching fiber was used in the initial work, leading to a 0.3-nm spectral resolution based on theoretical prediction. It is reasonable to conceive that more pulse stretching (i.e., a longer fiber) would be able to improve the spectral resolution. But the questions remain as to how much improvement can actually be achieved by adding more pulse-stretching fiber and what sets the upper limit of spectral resolution. In addition, the original TWOS spectrometer employs a separate delay line (1.38 km long with dispersion compensation) to construct a highly imbalanced Mach-Zehnder interferometer as part of the OSCAT scheme [14]. Given the fact that large dispersion is needed for pulse stretching anyway, such a configuration is clearly not the most efficient one.

In the work reported here, we upgrade the original TWOS spectrometer to address the above questions and deficiencies. A dual-function fiber delay line is introduced to perform both pulse delay and pulse stretching. We have also studied how fiber length impacts the total spectral range and the spectral resolution. Possible resolution-limiting factors are discussed and the corresponding solutions are presented.

II. Spectrometer Design

Fig. 1 shows the layout of our TWOS spectrometer. A mode locked fiber laser (Menlo Systems M-comb) generates a femtosecond pulse train at a center wavelength of 1540 nm and a repetition rate of 250 MHz. The laser has a 3-dB spectral width of about 60 nm, spanning from 1520 nm to 1580 nm as shown in Fig. 1 inset. The pulse repetition rate can be tuned by up to 2.5 MHz via an intracavity translation stage. In addition, fast modulation to the repetition rate can be made through a piezoelectric (PZT) actuator attached to one of the cavity mirrors [14]. The laser output is coupled into a highly

Manuscript received May 22, 2019; revised June 20, 2019; accepted July 7, 2019. Date of publication July 11, 2019; date of current version July 31, 2019. This work was supported in part by the National Science Foundation under Grant ECCS-1254902 and Grant ECCS-1606836. *(Corresponding author: Srikamal J. Soundararajan.)*

The authors are with the Department of Physics, The University of Alabama in Huntsville, Huntsville, AL 35899 USA (e-mail: ss0109@uah.edu).

Color versions of one or more of the figures in this letter are available online at http://ieeexplore.ieee.org.

Digital Object Identifier 10.1109/LPT.2019.2928228

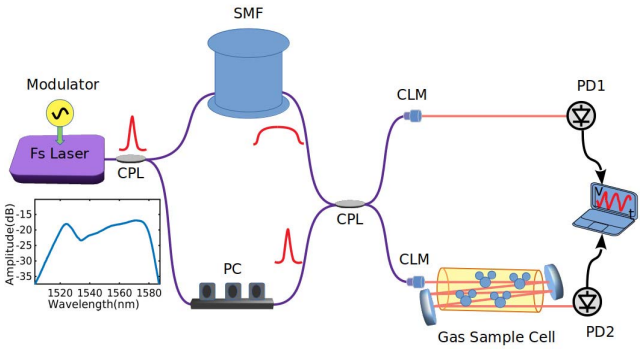

Fig. 1. System schematics of the OSCAT-based TWOS spectrometer, CLM: fiber collimator, CPL: fiber coupler, PC: polarization controller, and PD: photodetector. Inset: femtosecond laser spectrum.

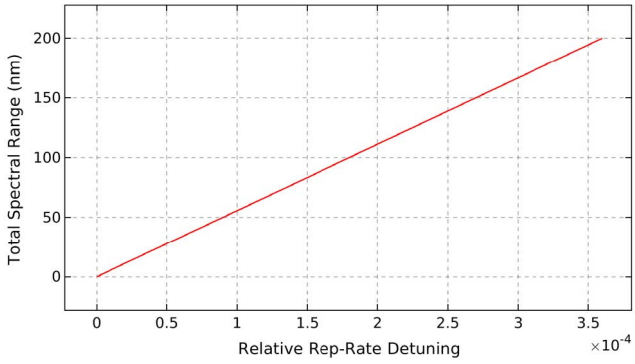

Fig. 2. The relation between total spectral range w_λ and relative repetition-rate detuning range $\Delta f_R/f_{R0}$ for a TWOS spectrometer with a dual-function optical delay line. $v_g = 2 \times 10^8$ m/s and $D = 18$ ps/nm· km are used here.

arm-length imbalanced Mach-Zehnder interferometer (MZI). The short arm of the MZI is about 5 m long, whereas the long arm consists of a fiber delay line ranging from 1 km to 3.9 km in length. The output of the MZI is split into two free-space paths. One beam is directly focused onto a photodetector to produce the *background* cross-correlation. The other beam picks up the atomic absorption through a multi-pass gas cell and converts it into the *signal* cross-correlation on a second photodetector. The two identical photodetectors are simple biased InGaAs detectors (Thorlabs DET20C). The two cross-correlation traces are compared numerically and the absorption spectrum of the specimen is extracted by means of a computer algorithm.

A subtle but important distinction between the current setup and the previously reported TWOS spectrometer [9] is that the delay line in the long arm is now composed of only single-mode fibers (SMF) rather than a combination of SMF and dispersion compensating fibers (DCF). This change allows the long arm to serve as both an optical delay line for OSCAT operation and a long pulse stretcher for wavelength-to-time mapping. It provides an elegant solution to the simultaneous need for long fibers in both OSCAT and TWOS. As a result of that, the system configuration has been further simplified. Yet the spectral resolution is significantly improved, as will be seen later.

The dual-function delay line also introduces a unique connection between pulse stretching and OSCAT pulse delay scan. This connection, along with its implication to the characteristics of the TWOS spectrometer will be discussed in the following section.

III. Spectral Range and Resolution

The operating principle of OSCAT has been elucidated in detail previously [14]. In essence, the method uses intracavity tuning to create a scan of repetition rate [10] and then converts it into a scan of relative pulse delay via a highly arm-length imbalanced interferometer [18]. For example, if the repetition rate is detuned by a *total* amount of Δf_R, the total change of pulse delay ΔT_d due to this detuning can be written as [14]

$$\Delta T_d = \frac{\Delta f_R \Delta L_i}{f_{R0} v_g}, \tag{1}$$

where f_{R0} is nominal repetition rate, ΔL_i is the interferometer arm-length difference, and v_g is pulse group velocity in fiber.

On the other hand, a femtosecond pulse entering the long arm of the MZI becomes an elongated pulse at the other end of the MZI (see Fig. 1), with the stretched pulse width $\Delta \tau_s$ given by [9]

$$\Delta \tau_s = |D| \, l_s \, \Delta \lambda, \tag{2}$$

where D is fiber group-velocity dispersion (GVD) parameter, l_s is the total length of pulse-stretching fiber, and $\Delta \lambda$ is pulse spectral width. This relation clearly shows the linear mapping from spectral domain to time domain by fiber dispersion. For a TWOS spectrometer, a relevant question is: how much of the stretched pulse can be sampled by the reference pulses? This is important because only those spectral features that fall into the sampling window can be read out by the spectrometer. To answer this question, it is worth pointing out that, with the long arm serving as a *dual-function* delay line, the MZI arm-length difference is approximately equal to the stretching fiber length, i.e., $\Delta L_i \approx l_s$. Taking the ratio of (1) and (2) then leads to the relation

$$w_\lambda \equiv \frac{\Delta T_d}{\Delta \tau_s} \Delta \lambda = \frac{\Delta f_R}{v_g \, |D| \, f_{R0}}, \tag{3}$$

where w_λ represents the spectral window that can be sampled by the spectrometer. The right-hand side of (3) shows how this window is determined by fiber and modulation parameters. It is interesting to notice that the total spectral range of the spectrometer is independent of the delay line length l_s. This is fundamentally a manifestation of the dual-function nature of the long arm.

Meanwhile, the typical spectral resolution of an OSCAT-based TWOS spectrometer has been found to be [9]

$$\delta \lambda_{\text{TWOS}} = \frac{\Delta \tau_r}{|D| \, l_s}, \tag{4}$$

where $\Delta \tau_r$ is the reference pulse width. The fact that w_λ is independent of l_s whereas $\delta \lambda_{\text{TWOS}}$ is inversely proportional to l_s allows these two parameters to be optimized independently, which can be a useful feature in system development. Fig. 2 shows a quantitative example of (3), where w_λ is plotted

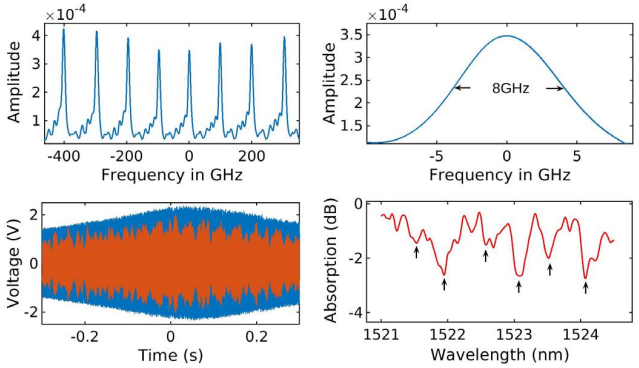

Fig. 3. Spectral measurement results: (a) The transmission spectrum of a fiber Fabry-Perot (FP) cavity, (b) the close-in profile of a FP resonance peak, (c) A time-domain trace produced by a 50-torr C_2H_2 gas sample, and (d) absorption peaks of C_2H_2 near 1523 nm measured by the TWOS spectrometer.

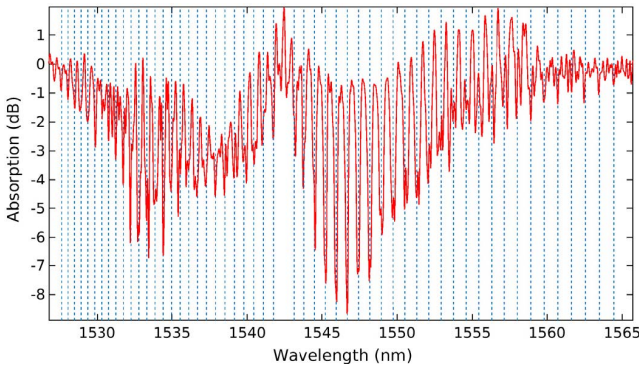

Fig. 4. The absorption spectrum of hydrogen cyanide measured by the TWOS spectrometer. Light-colored (dashed) grids represent HITRAN data.

against the relative repetition-rate detuning $\Delta f_R/f_{R0}$. Typical values of $v_g = 2 \times 10^8$ m/s and $D = 18$ ps/nm· km for SMF have been used in this case. For a TWOS spectrometer to achieve a 100-nm spectral range, a repetition-rate detuning of $\Delta f_R/f_{R0} = 1.8 \times 10^{-4}$ is sufficient. In the case of our current system, with $f_{R0} = 250$ MHz, the required Δf_R is 45 kHz, which is well within the available intracavity tuning range.

IV. Experimental Results

Spectral measurements have been made using our TWOS spectrometer with various optical devices and atomic samples. Fig. 3 summarizes some of these results. Fig. 3(a) shows the measured transmission spectrum of a fiber Fabry-Perot cavity, which has a free-spectral range of about 100 GHz. Periodical resonance peaks are clearly resolved. These peaks are used to calibrate the spectral resolution of the spectrometer. Fig. 3(b) shows the profile of one of the resonance peaks, where a resolution-limited linewidth of 8 GHz has been measured.

The spectrometer has been used to measure the absorption spectrum of acetylene (C_2H_2) in the near infrared region at a pressure of 50 torr. A sample of the recorded time-domain trace is shown in Fig. 3(c), where the dark background and the corrugated foreground traces are measured by PD1 and PD2 in Fig. 1, respectively. The extracted absorption spectrum is shown in Fig. 3(d), where absorption peaks can be clearly identified.

To demonstrate the capability of the TWOS spectrometer in making accurate measurement of spectral features within a broad range, we have measured the entire R branch and P branch of the absorption spectrum of hydrogen cyanide (HCN) in the near infrared wavelength region, which spans over a 40-nm breadth (1525–1565 nm). The spectrometer is able to resolve every single absorption line within this range as shown in Fig. 4. Moreover, excellent agreement has been achieved with the HITRAN-documented spectral lines, shown here as the light-colored grids.

V. Discussion and Conclusion

Experiments with different lengths of the pulse-stretching fiber l_s have shown independence of the total spectral range w_λ versus l_s, which is in agreement with (3). However, the measured spectral resolution appears to deviate from the prediction of (4) by a sizeable margin. The 8-GHz resolution (~60 pm) shown in Fig. 3(b) is measured with a 3-km SMF delay line. But a resolution of similar scale is also obtained with a 1-km delay line in the HCN measurement shown in Fig. 4. In fact, no significant improvement of spectral resolution has been observed when the delay-line length is over 400 m. According to (4), using an estimated reference pulse width of 400 fs and a typical SMF GVD parameter of $D = 18$ ps/nm· km, a nominal value of 70 pm is estimated for $\delta\lambda_{\mathrm{TWOS}}$. This is approximately the same as the result obtained with a 3-km delay line. So the question is: what prevents further improvement of spectral resolution as the delay line extends beyond 400 m? One conceivable factor is the coherence length of the laser. A typical femtosecond comb laser has a free-run linewidth on the order of hundreds of kilohertz [19]. Taking a nominal value of 500 kHz, the corresponding coherence length is 400 m in fiber. Since both PD1 and PD2 in our current TWOS spectrometer are linear detectors, the measured cross-correlation signals are essentially the interference patterns produced by the imbalanced MZI (see Fig. 1). When the arm-length difference of the MZI is greater than the coherence length of the laser, the contrast of the fringes begins to drop and the signal becomes increasingly noisy. This eventually may become the limiting factor for spectral resolution. There are, however, ways to mitigate the impact of coherence length. Using nonlinear detectors rather than linear detectors permits the measurement of *intensity* cross-correlation (instead of field cross-correlation in the current case), which is less susceptible to field coherence. Alternatively, one can also use pulse lasers with ultra-narrow spectral lines such as comb lasers based on electro-optic modulations, whose linewidths are typically on the order of kHz [20].

In conclusion, we have demonstrated a time-stretch spectrometer based on the OSCAT scheme. A km-scale dual-function fiber-optic link serves as both a pulse stretcher and a long delay line in an imbalanced MZI. The total spectral range is found to be independent of the delay line length. Spectral resolution as small as 8 GHz has been achieved. Limited laser coherence length along with the linear detection scheme used in the current setup are considered likely limiting factors for

such a resolution. Possible solutions include using nonlinear detectors or frequency comb lasers with narrow spectral lines.

REFERENCES

[1] R. R. Thomson, "Time-stretch spectroscopy STEAMs ahead," *Laser Focus World*, vol. 53, no. 10, pp. 41–45, Oct. 2017.

[2] A. Mahjoubfar, D. V. Churkin, S. Barland, N. Broderick, S. K. Turitsyn, and B. Jalali, "Time stretch and its applications," *Nature Photon.*, vol. 11, pp. 341–351, Jun. 2017.

[3] K. Goda and B. Jalali, "Dispersive Fourier transformation for fast continuous single-shot measurements," *Nature Photon.*, vol. 7, pp. 102–112, Jan. 2013.

[4] J. Chou, Y. Han, and B. Jalali, "Time-wavelength spectroscopy for chemical sensing," *IEEE Photon. Technol. Lett.*, vol. 16, no. 4, pp. 1140–1142, Apr. 2004.

[5] J. Hult, R. S. Watt, and C. F. Kaminski, "High bandwidth absorption spectroscopy with a dispersed supercontinuum source," *Opt. Express*, vol. 15, no. 8, pp. 11385–11395, Sep. 2007.

[6] J. Chou, D. R. Solli, and B. Jalali, "Real-time spectroscopy with subgigahertz resolution using amplified dispersive Fourier transformation," *Appl. Phys. Lett.*, vol. 92, no. 11, Mar. 2008, Art. no. 111102.

[7] A. S. Bhushan, P. Kelkar, and B. Jalali, "30 Gsample/s time-stretch analogue-to-digital converter," *Electron. Lett.*, vol. 36, no. 18, pp. 1526–1527, Aug. 2000.

[8] D. R. Solli, J. Chou, and B. Jalali, "Amplified wavelength–time transformation for real-time spectroscopy," *Nature Photon.*, vol. 2, pp. 48–51, Dec. 2007.

[9] S. J. Soundararajan, L. Yang, S. Zhang, H. Jani, and L. Duan, "Time-wavelength optical sampling spectroscopy based on dynamic laser cavity tuning," *J. Opt. Soc. Amer. B, Opt. Phys.*, vol. 35, no. 5, pp. 1186–1191, May 2018.

[10] L. Duan and L. Yang, "Ultrafast optical sampling finds applications in precision measurement," *J. Sci. Ind. Metrol.*, vol. 1, no. 1, pp. 1–5, Feb. 2016.

[11] A. Bartels *et al.*, "Ultrafast time-domain spectroscopy based on high-speed asynchronous optical sampling," *Rev. Sci. Instrum.*, vol. 78, no. 3, 2007, Art. no. 035107.

[12] T. Hochrein, R. Wilk, M. Mei, R. Holzwarth, N. Krumbholz, and M. Koch, "Optical sampling by laser cavity tuning," *Opt. Express*, vol. 18, no. 2, pp. 1613–1617, Jan. 2010.

[13] S. Potvin, S. Boudreau, J.-D. Deschênes, and J. Genest, "Fully referenced single-comb interferometry using optical sampling by laser-cavity tuning," *Appl. Opt.*, vol. 52, no. 2, pp. 248–255, Jan. 2013.

[14] L. Yang, J. Nie, and L. Duan, "Dynamic optical sampling by cavity tuning and its application in lidar," *Opt. Express*, vol. 21, no. 3, pp. 3850–3860, Feb. 2013.

[15] S. Boudreau and J. Genest, "Range-resolved vibrometry using a frequency comb in the OSCAT configuration," *Opt. Express*, vol. 22, no. 7, pp. 8101–8113, Apr. 2014.

[16] L. Yang and L. Duan, "Depth-resolved imaging based on optical sampling by cavity tuning," *IEEE Photon. Technol. Lett.*, vol. 27, no. 16, pp. 1761–1764, Aug. 15, 2015.

[17] K. Lee *et al.*, "Fourier-transform spectroscopy using an Er-doped fiber femtosecond laser by sweeping the pulse repetition rate," *Sci. Rep.*, vol. 5, Oct. 2015, Art. no. 15726.

[18] M. I. Kayes and M. Rochette, "Fourier transform spectroscopy by repetition rate sweeping of a single electro-optic frequency comb," *Opt. Lett.*, vol. 43, no. 5, pp. 967–970, Mar. 2018.

[19] N. R. Newbury and W. C. Swann, "Low-noise fiber-laser frequency combs," *J. Opt. Soc. Amer. B, Opt. Phys.*, vol. 24, no. 8, pp. 1756–1770, Aug. 2007.

[20] M. I. Kayes and M. Rochette, "Optical frequency comb generation with ultra-narrow spectral lines," *Opt. Lett.*, vol. 42, no. 14, pp. 2718–2721, Jul. 2017.